



Paper-like N-doped graphene films prepared by hydroxylamine diffusion induced assembly and their ultrahigh-rate capacitive properties



Yunzhen Chang, Gaoyi Han*, Dongying Fu, Feifei Liu, Miaoyu Li, Yanping Li, Cuixian Liu

Institute of Molecular Science, Key Laboratory of Chemical Biology and Molecular Engineering of Education Ministry, Shanxi University, Taiyuan 030006, China

ARTICLE INFO

Article history:

Received 30 August 2013
Received in revised form 25 October 2013
Accepted 27 October 2013
Available online 11 November 2013

Keywords:

Graphene
N-doped
Capacitor
Hydroxylamine
Assembly

ABSTRACT

An approach as “hydroxylamine diffusion induced assembly” has been developed to fabricate N-doped graphene paper-like films (NG-P) and composite films containing multiwalled carbon nanotubes (NG-MWCNT-P). The obtained films have been characterized by using X-ray photoelectron spectroscopy, X-ray diffraction spectroscopy and scanning electron microscopy. The results indicate that the N atoms have doped into the graphene sheets and the interplanar distance between the graphene sheets decreases with the increment of the thermally treated temperature. The films of NG-P prepared at 100 °C are flexible and exhibit a maximum tensile stress of about 70.5 MPa and a Young's modulus of about 17.7 GPa, and the films of NG-P thermally treated at 300 °C (NG-P300) have high thermal conductivity of about 3403 W m⁻¹ K⁻¹. However, the NG-MWCNT-P film exhibits a relatively weaker tensile stress compared with NG-P. The electrochemical measurements show that the NG-P300 possesses excellent ultrahigh-rate capacitive properties, and that the specific capacitance and the impedance phase angle of the capacitor can reach to about 318 μF cm⁻² and -77.1° respectively at frequency of 120 Hz. Simple measurements on NG-MWCNT-P show that it has specific capacitance of about 90 F g⁻¹ based on one electrode and the capacitor possesses the high-rate capability.

© 2013 Elsevier Ltd. All rights reserved.

1. Introduction

Graphene, a kind of two-dimensional carbon material constructed by layers of sp²-bonded carbon, exhibits applications in such fields as electronics [1], composite materials [2–5], catalysis [6,7], energy generation [8,9] and storage [10–12] owing to its extremely mechanical strength, exceptionally high electrical conductivity and thermal conductivities [13–15]. The graphene produced through chemically reducing graphene oxide (GO, obtained from graphite) is considered to be the simpler, more effective and inexpensive approach to achieve large-scale use [16] although methods of mechanical exfoliation, epitaxial growth and chemical vapor deposition [17,18] can be used to prepare high-quality graphene. However, chemically reduced GO (rGO) dissolved in water will occur an irreversible coagulation, which has blocked to fabricate bulk graphene-based materials from rGO.

Up to date, considerable efforts have devoted to prepare or assemble graphene micro-/nano-architectures in order to extend their applications. For example, graphene paper-like films have

been prepared by two-step method: GO films are prepared by vacuum filtration or liquid-air assembly firstly, and then the GO films are reduced by reducing agent or thermal treatment [19–21]. However, the lack of a simple, general and technologically feasible route to produce graphene films with large area is still a major obstacle for large-scale applications. Besides the morphology control, chemical doping and etching are other effective approaches to tailor the properties of graphene and greatly expand the applications [22]. Among numerous potential dopants, N is considered to be an excellent element because of its comparable atomic size and five valence electrons available to form strong valence bonds with C atoms. Compared with the N-doping approaches performed under harsh conditions such as chemical vapor deposition, segregation growth, arc-discharge and plasma treatment [23–26], N-doped graphene synthesized by solution-phase process is considered to be the feasible approach due to its simplicity, low-cost and larger-scale production [27–29]. Hydroxylamine as N source possesses relatively lower toxic properties than the widely-used hydrazine hydrate [30], but it is rarely used as the chemical reductant and dopant to prepare N-doped graphene [31].

It is well known that GO can be considered as a kind of macromolecule with hydroxyl and epoxide functional groups on the basal plane, carbonyl and carboxyl groups at the edge [32,33].

* Corresponding author. Tel.: +86 351 7010699; fax: +86 351 7016358.
E-mail address: han.gaoyis@sxu.edu.cn (G. Han).

The dispersion of GO can be coagulated under the action of salt, acid, base and other reagents. For example, the oxygen-containing groups of GO can interact with reagents containing amine or hydroxyl groups to form precipitate or gel. Furthermore, two kind of liquids or solutions with different densities can not quickly blend when the heavy liquid is carefully injected into the bottom of the light liquid without stirring even if the both liquids are miscible, for example water and ethanol.

According to the above-mentioned factors, we can develop a feasible approach named as “hydroxylamine diffusion induced assembly (DIA)” to prepare N-doped graphene paper-like films in large scale. Using this process, the N-doped graphene films will be conveniently produced by directly injecting GO suspension into the bottom of ethanol solution of hydroxylamine, then the GO coagulate slowly to form shaped assembly at room temperature with the help of hydroxylamine flocculants, finally the desired N-doped graphene films are obtained after the evaporation of the solvent under heating. Up to the present, the researches on the ultrahigh-rate capacitive properties of paper-like graphene films are still rare [34–36] although many literatures have focused on their mechanic properties or use on substrates [2,19–21]. In this paper, the paper-like N-doped graphene (NG-P) films have been prepared through DIA process and the materials have been characterized and their capacitive properties have also been measured in detail.

2. Experimental

2.1. Materials

Natural graphite powder (325 mesh) was purchased from Tianjin Guangfu Research Institute. Hydroxylamine hydrochloride was obtained from Tianjin North Fine Chemical Co., Ltd., and all other chemicals were of analytical grade. GO was prepared by oxidizing the natural graphite powder according to the method reported in literatures [7,19], the GO dispersion was diluted to about 5.0 mg mL^{-1} and treated under the ultrasonication for 10 min before use. Hydroxylamine was generally prepared by reacting equal molar hydroxylamine hydrochloride with potassium hydroxide in ethanol solution and used instantly (see Supporting Information).

2.2. Fabrication of the NG-P films

Ethanol solution of hydroxylamine (300 mL, 0.5 mg mL^{-1}) was poured into a container ($20.5 \times 20.5 \times 5 \text{ cm}$, length \times width \times height) containing a square glass plate with a thickness of 1.1 mm at the bottom. The container was placed into an oven and then adjusted to leveling, and 60.0 mL GO dispersion (5.0 mg mL^{-1}) was then injected into the bottom of the ethanol solution through a glass tube carefully. Subsequently, the container was placed for more than 6.0 h at room temperature, during which the GO sheets were assembled into gel slowly. The temperature of the oven was firstly increased to about 40°C slowly and kept at this temperature for about 1.0 h. Subsequently, the temperature was raised to 100°C and kept this temperature until the thickness of the solution in container was about 1.0 mm. The film of NG-P deposited on the glass was removed from the container and heated at 100°C for 10 h after the solution was evaporated completely. Finally, the film was peeled from the glass substrate carefully and heated at 150°C for 5 h and 300°C for 2 h further, and washed by distilled water thoroughly. The samples as-prepared at 100, 150 and 300°C were named as NG-P100, NG-P150 and NG-P300, respectively. The films of NG-P300 with different thickness were also fabricated by using the same process through controlling the concentration of

the injected GO solution. For comparison, GO film was fabricated by using the air-solution assembly method according to literature [20], and then graphene film named as G-P300 was obtained by heating the GO film at 300°C under nitrogen atmosphere.

2.3. Fabrication of the composite films of N-doped graphene and multiwalled carbon nanotubes (NG-MWCNT-P)

In order to verify the effectiveness of DIA for composites, the film of NG-MWCNT-P was prepared by using the similar process. Briefly, 100 mL ethanol solution of hydroxylamine (0.5 mg mL^{-1}) was poured into a container ($10.5 \times 10.5 \times 5 \text{ cm}$, length \times width \times height) containing a square glass plate with a thickness of 1.1 mm at the bottom. The container was placed into an oven and then adjusted to leveling. Then 20.0 mL mixture of GO (4.0 mg mL^{-1}) and MWCNTs (1.0 mg mL^{-1}) was injected into the bottom of the ethanol solution through a glass tube carefully. After the layer of GO and MWCNTs has assembled and formed gel (standing for 6.0 h or long), the temperature of the oven was increased to 40°C and kept this temperature for 2.0 h, the temperature was then increased to about 110°C to evaporate most of the solvent. Successively the temperature was adjusted to 70°C and kept at this temperature until the surface of the composite paper has become dried. The sample together with the glass substrate was carefully removed from the container and heated at 100°C for 10 h. Finally, the composite film was peeled from the glass substrate carefully and heated at 150°C for 5 h further, and washed by distilled water thoroughly. The samples prepared at 100 and 150°C were named as NG-MWCNT-P100, NG-MWCNT-P150, respectively.

2.4. Characterization and Measurements

Atomic force microscopic (AFM) images were taken out using a Nanoscope III Multi Mode SPM (Digital Instruments) with an AS-12 (“E”) scanner operated in tapping mode in conjunction with a V-shaped tapping tip (Applied Nanostructures SPM model: ACTA), and the images were recorded at scan rate of 2 Hz. The X-ray diffraction (XRD) patterns of the products were recorded on a Bruker D8 Advance X-ray diffraction meter with $\text{Cu K}\alpha$ radiation and graphite monochromator at the scan speed of 5° min^{-1} with a step size of 0.02° . The morphologies of the samples were observed by using a JEOL-JSM-6701 field-emission microscope (SEM) operating at an accelerating voltage of 10 kV. X-ray photoelectron spectroscopy (XPS) measurements were performed with an ESCAL-ab 220i-XL spectrometer (VG Scientific, England) using a monochromic Al K α source at 1486.6 eV. Mechanical tests were conducted with an electronic stretching machine (INSTRON test machine 5544). The samples were clamped by using the film clamps with a clamp compliance of about $0.2 \mu\text{m N}^{-1}$. All tensile tests were performed in controlled force mode with a preload of 0.001 N and at a strain ramp rate of 0.2 mm min^{-1} . Tensile modulus is determined by fitting the stress-strain plot in the “elastic” regime with a straight line. The thermal conductivities of the samples were measured on a Netzsch LFA 447 nanoflash TM instrument at room temperature.

The fabrications of the capacitors were described as follows: two pieces of nearly identical (in weight and size) NG-P, G-P300 or NG-MWCNT-P were separated by a filter paper soaked with 1.0 M H_2SO_4 or 25% KOH aqueous solution. Before the electrochemical measurements, the slices of N-doped graphene materials were also immersed in electrolyte solution under vacuum in order to make the electrolyte exchange their interior. Two Pt foils were used as the current collectors. All the components were assembled into a sandwiched structure between the two plastic sheets and the structural scheme of the capacitor was showed in Fig. S1. Electrochemical performances of the cells were tested by cyclic voltammetry

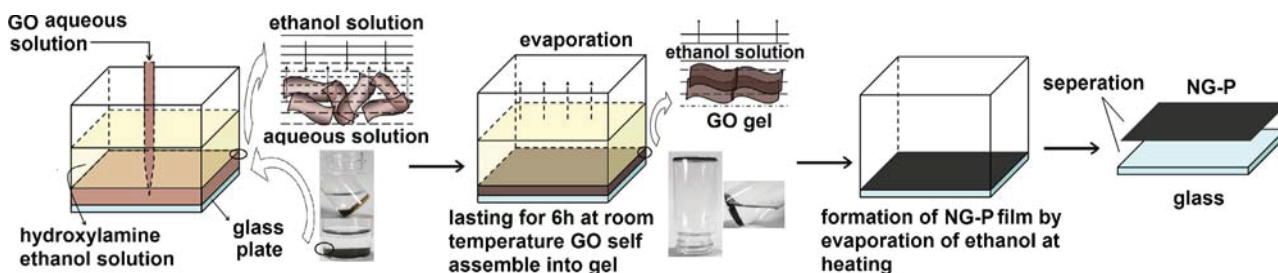


Figure 1. The schematic diagram of the “hydroxylamine diffusion induced assembly” for preparation of N-doped graphene paper-like films.

(CV), galvanostatic charge/discharge method and electrochemical impedance spectroscopy (EIS) on a CHI660 C electrochemistry workstation (Chenhua, Shanghai). The EIS tests were carried out in the frequency range of 10^5 – 10^{-2} Hz at the amplitude of 5 mV referring to open circuit potential.

3. Results and discussion

3.1. The process of DIA

Fig. 1 shows the schematic illustration of the process for preparation of the films of NG-P, briefly, the GO dispersion is carefully injected into the bottom of the container filled with ethanol solution of hydroxylamine which acts as a coagulation, N-source and reducer during the process. With the mutual diffusion of water and ethanol, hydroxylamine molecules diffuse into the GO layer gradually and interact with GO sheets, and then the orientation of GO sheets becomes more ordered than the beginning. Subsequently, the GO assembly or gel was formed at room temperature after several hours with the decrease of water and the increase of hydroxylamine in the GO layer. Finally, the NG-P will be obtained by evaporating the solvent at 100°C . The thickness of NG-P can be adjusted by the concentration of the GO solution.

3.2. Characterization of the products

As shown in Fig. 2, it can be seen that the as-prepared GO exhibits a wide dimensional distribution, and that the size of the GO sheets is

ranged from tens of nanometers to more than one micrometer. The thickness of the GO sheets is measured to be about 0.80 nm, which is larger than the interplanar distance of the graphite due to the oxygen-containing groups on the sheets [9]. The data on the basis of XPS show that GO contains a relatively high O content (33.1%) in atom (Fig. S2), and that the C/O ratio is calculated to be about 2.04.

The NG-P100 with large area (Fig. 3A, 18×18 cm) prepared by DIA is flexible and can be easily folded without destroying the structure and sheared into the patterns of double happiness characters and panda by using Chinese kirigami (Fig. 3B and C). Using the process of DIA, the composite films of NG-MWCNT-P can also be conveniently prepared by using the mixture of GO and MWCNTs as injecting solution (Fig. 3D), but only relatively small films with a size of 8.5×8.5 cm can be obtained due to the crack caused by the addition of MWCNTs during drying process. The surface of the NG-P (Fig. 4A) is rough and exhibits some creases or pores, but the specific surface area of the NG-P measured by BET is only about $4.4 \text{ m}^2 \text{ g}^{-1}$ for NG-P100 and $2.2 \text{ m}^2 \text{ g}^{-1}$ for NG-P300, which indicates that the NG-P are compact and the pores only exhibit on the surface of the films. The transverse SEM images show that the film exhibits the lamellar structure and the layers are stacked closely, which are similar to other paper-like graphene films reported previously [16–18]. Compared with NG-P100 (Fig. 4B), NG-P300 (Fig. 4C) shows clearer lamellar structure, which may indicate that NG-P300 exhibits higher electrical conductivity than NG-P100. However, the surface of NG-MWCNT-P exhibits some MWCNTs and pores (Fig. 4D). From TEM image and the transverse SEM image shown in

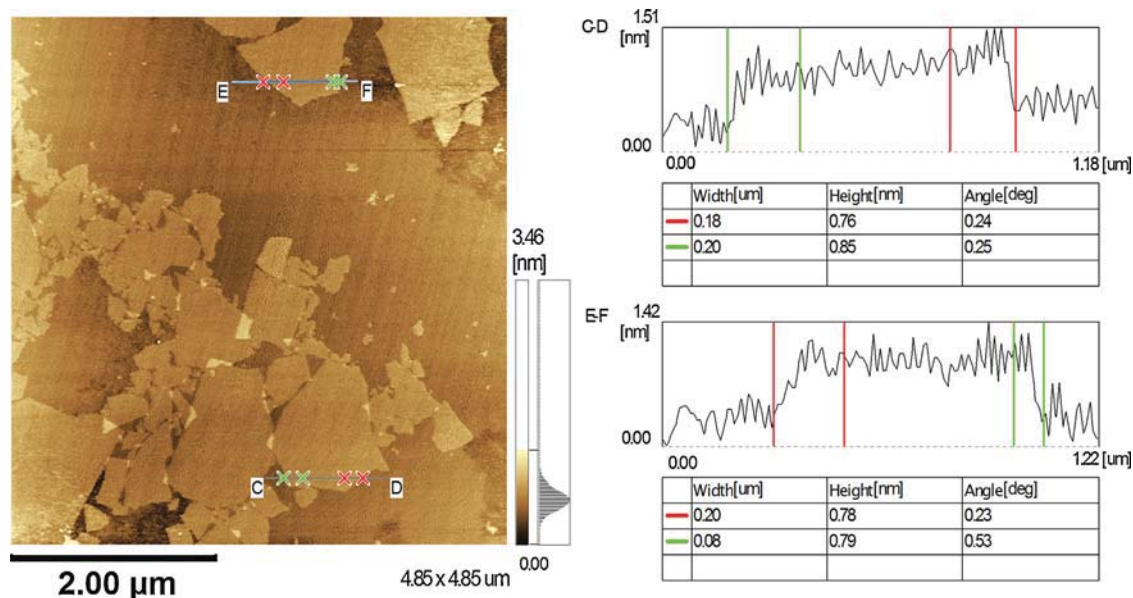


Figure 2. The AFM image of the as-prepared GO.

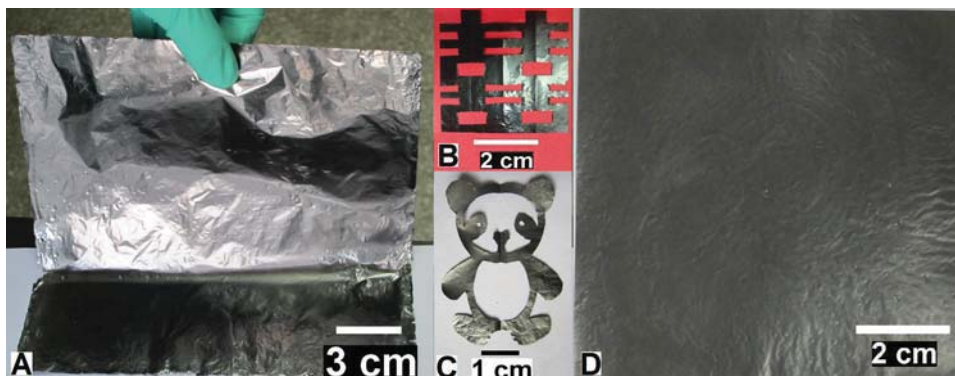


Figure 3. The photograph of NG-P with large area (A), the patterns of double happiness characters and panda sheared from NG-P by Chinese kirigami (B and C), and the photograph of NG-MWCNT-P with large area (D).

Fig. 4E and F, it can be clearly found that the MWCNTs dispersed between the layers of graphene in NG-MWCNT-P. This indicates that the process of DIA can be used to prepare not only graphene films but also its composite films.

Compared with the XPS spectrum of GO, the samples of NG-P show relatively stronger C1s and weaker O1s XPS peaks. It is interesting to find that the spectra present weak N1s XPS for samples of NG-P, which indicates that the N atom has doped into the graphene sheets at relatively low reaction temperature (Fig. 5A). Furthermore, the content of the elements of C, O and N has changed when the samples of NG-P are treated at different temperatures. For example, the values of the C: O: N for NG-P100, NG-P150 and NG-P300 based on XPS are calculated to be about 1.00: 0.19: 0.062, 1.00: 0.17: 0.047 and 1.00: 0.14: 0.033, respectively. From the above data, it is found that the C/O ratio increases from 2.04 for GO to about 5.26, 5.88 and 7.14 for NG-P100, NG-P150 and NG-P300,

respectively. These results indicate that the GO has been reduced during the process and that the content of N atom in the NG-P decreases with the increment of treating temperature.

From the high-resolution C1s XPS spectra (Fig. 5B), it is found that the peaks of C1s for NG-P are very different from that of GO. The peaks corresponding to C-O bond in NG-P (located at high binding energy region) have become weaker obviously compared with GO, indicating that the oxygen-containing groups have been reduced and the non-conjugated structures have converted to the π -conjugated graphene structures. The six fitted peaks located at about 284.48, 284.87, 285.63, 286.54, 287.54 and 288.61 eV can be assigned to the C=C, C-C, C=N, C-OR, C=O and COOR groups [33], respectively. The samples of NG-P150 and NG-P300 show the similar C1s XPS peaks, but the relative contents of the groups are different (Table S1).

It is reported that the binding energy of pyridinic N, pyrrolic N, quaternary N and the N-oxides of pyridinic N is located at about

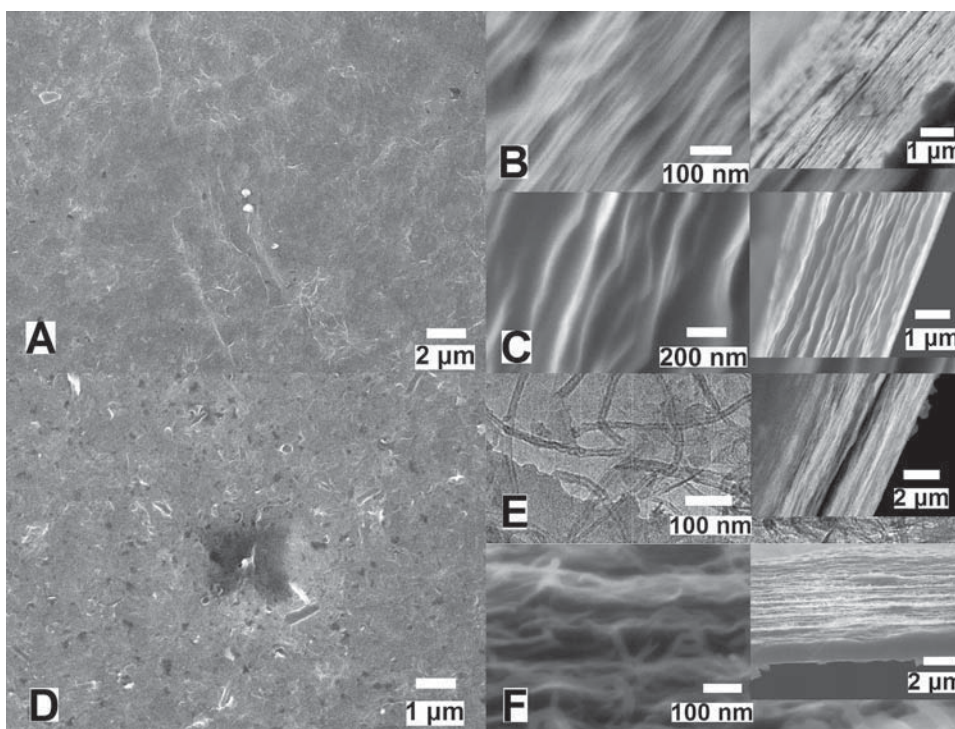


Figure 4. The SEM image of the NG-P's surface (A) and the transverse section SEM image of NG-P100 (B) and NG-P300 (C), the SEM image of NG-MWCNT-P's surface (D), the TEM image of NG-MWCNT-P100 (E, the inserted figure: the transverse section SEM image) and the transverse section SEM images of NG-MWCNT-P150 (F). The inserted figures are the SEM image in low magnification.

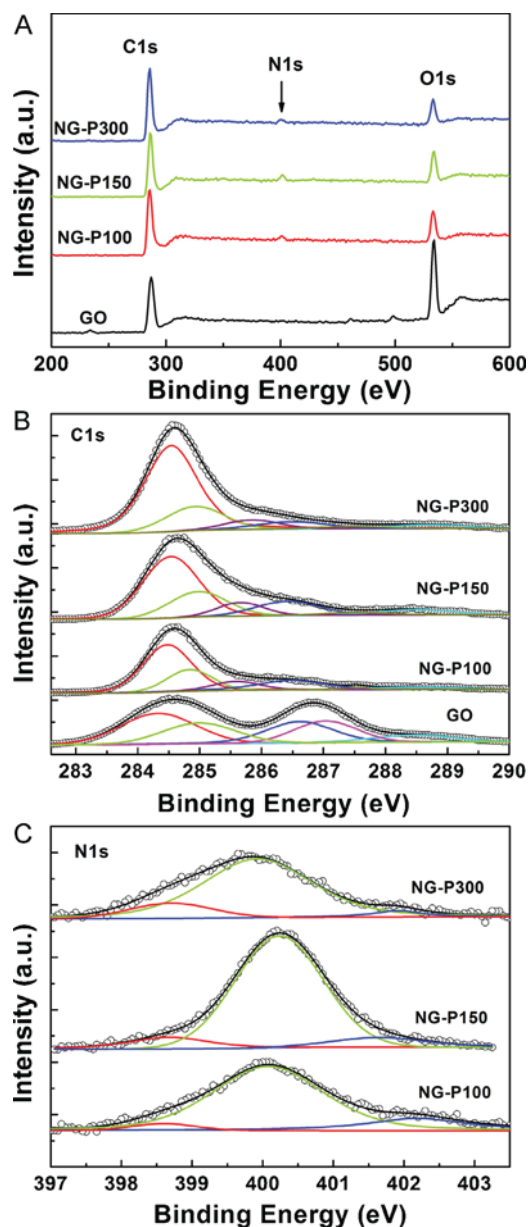


Figure 5. The XPS spectra of samples: (A) whole spectra, (B) C1s and (C) N1s XPS spectra.

398.1–399.3, 399.8–401.2, 401.1–402.7 and 402.8 eV [22], respectively. Therefore, the fitted XPS peaks of N1s in samples of NG-P (Fig. 5C) are assigned to pyridinic (398.6 eV), pyrrolic (399.8 eV) and quaternary N (402.1 eV), which is consistent with literature [31], indicating that the N atom has doped into the NG-P when the GO reacts with the hydroxylamine during the process. From the content of different types of N atom listed in Table 1, it is found that the proportion of quaternary-type N decreases while the content of pyridinic and pyrrolic-type N remarkably increases with

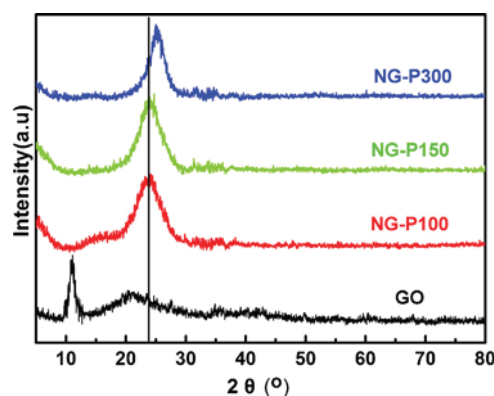


Figure 6. The XRD patterns of the samples.

the increase of the thermally treating temperature, which indicates that the part of quaternary N such as $R-NH_3^+$ has been converted to pyrrolic and pyridinic N. The possible N insertion pathway in the graphene sheets is thought to be similar to the literature reported previously [31]. Furthermore, it is found that the composite films of NG-MWCNT-P contains the elements of C, O, N and S, which indicates that N has also doped into the graphene sheets while the S signals come from MWCNTs which have been activated by mixture of nitric acid and sulfuric acid (Fig.S5–7, Table S2 and 3).

From the XRD patterns (Fig. 6), it is clear that the GO exhibits two diffraction peaks, one is located at about 10.5° and the other at about 21.0° , the distance between the layers of GO sheets is calculated to be about 0.797 and 0.397 nm according to Bragg equation ($2d\sin\theta=n\lambda$). However, the peak at small angle has disappeared in the NG-P samples, and the distance between the layers of NG-P is calculated to be about 0.372 nm for NG-P100, 0.371 nm for NG-P150, and 0.356 nm for NG-P300, which indicates that the reduction of the GO make the interplanar distance become small, and that the high treating temperature makes the interplanar distance more smaller due to the further elimination of the oxygen containing groups. But the distance between the layers is still larger than that of graphite (0.335 nm).

The NG-P100 possesses a tensile stress of about 70.5 MPa and Young's modulus of about 17.7 GPa, while NG-MWCNT-P100 only exhibits a tensile stress of about 17.9 MPa and a Young's modulus of about 13.3 GPa (Fig. 7A). However, the tensile stress decreases dramatically with the increment of treated temperature while Young's modulus has only slight change (Fig. 7B). For example, the NG-P150 possesses a tensile stress of about 18.9 MPa and a Young's modulus of about 17.5 GPa while the NG-MWCNT-P150 exhibits a tensile stress of about 15.5 MPa and Young's modulus about 14.2 GPa. The literatures [19,20] have reported that the stronger mechanical properties of GO paper are mainly derived from the unique interlocking-tile arrangement of the nanoscale GO sheets through the strong interactions of carboxyl and hydroxyl groups. However, the high temperature will eliminate the carboxyl and hydroxyl groups in the films, therefore the NG-P and NG-MWCNT-P prepared at lower temperature have a stronger tensile strength than the samples treated at higher temperature.

Table 1

The relative contents of different N atom of NG-P treated at different temperatures.

Type of N atom	NG-P100	NG-P150	NG-P300
	Position (eV)	Content (at.%)	Position (eV)
Pyridinic N	398.58	4.17	398.69
Pyrrolic N	400.01	78.4	400.21
Quaternary N	402.07	17.4	401.74
	Content (at.%)	Position (eV)	Content (at.%)
	10.3	398.68	13.8
	80.6	399.91	81.2
	9.14	401.93	4.94

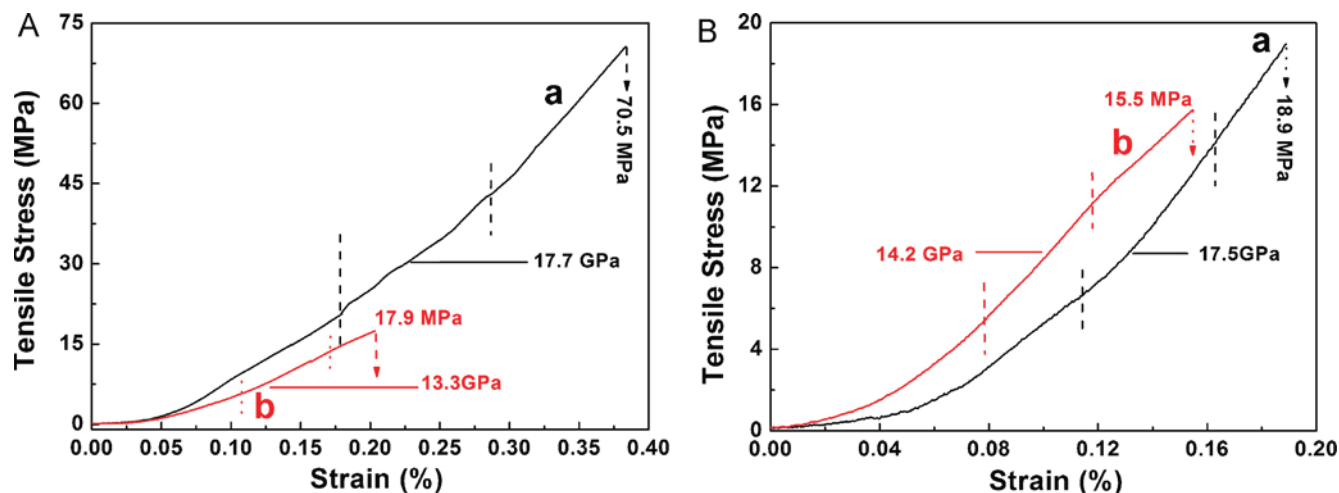


Figure 7. The mechanic property of the NG-P (a) and NG-MWCNT-P (b) prepared at 100 °C (A) and 150 °C (B).

The electrical conductivities are measured by using four-probe technique and found to be about 3.2, 5.8 and 32.6 Scm^{-1} for the sample of NG-P100, NG-P150 and NG-P300, respectively. It is well known that the conductivity of graphene prepared from GO is strongly depended on the C/O ratio and that the conductivity increases with the increment of C/O value. Therefore high treated temperature is favorable to increase the conductivity due to the increase of C/O ratio. It has been proved that graphene materials has excellent thermal conductivities, so the thermal conductivities of the NG-P samples are measured at room temperature and found to be about 2232 and 3403 $\text{Wm}^{-1}\text{K}^{-1}$ for NG-P100 and NG-P300, respectively (Fig. S8 and Table S4). These results may be resulted from the good arrangement of the graphene sheets and can be comparable to the results reported in literature [15].

3.3. The electrochemical properties

The CV curves of the capacitors assembled by the films of NG-P are recorded in 1.0M H_2SO_4 electrolyte and shown in Fig. 8. It is clear that the CV curves of the capacitors assembled by NG-P100, NG-P150 and NG-P300 show quasi-rectangular like profiles from the scan rates of 5.0 to 800 Vs^{-1} . It is interesting to find that the capacitors assembled by NG-P300 possess more rectangular CV profiles and larger current density than that by NG-P150 and NG-P100 at the large scan rates, which indicates that the NG-P300 exhibits better ultra-fast capacitive properties than other [35]. This may be because NG-P300 has larger electrical conductivity and small interplanar spacing distance than NG-P150 and NG-P100. The CV curves shown in Fig. 9 reveal that the capacitor fabricated by G-P300 also exhibits the quasi-rectangular like profiles from scan rates of 5.0 to 800 Vs^{-1} . However, it exhibits less rectangular CV profiles and smaller current density than the NG-P at the same large scan rates, indicating that it has small specific capacitance (C_{sc}) at large scan rates.

In order to further evaluate the capacitive properties of the NG-P films, the C_{sc} values on the basis of one electrode at different scan rates have been calculated based on the CV curves and shown in Fig. 10. It is clear that the NG-P100 has the largest while the NG-P300 has the smallest C_{sc} at small scan rates. However, the NG-P300 has the larger C_{sc} than NG-P150 and NG-P100 at large scan rates. It is interesting to find that G-P300 possesses smaller C_{sc} values than the samples of NG-P at large scan rates. The C_{sc} values decrease with the increment of the scan rates, but

the trend of decrease for NG-P300 is much slighter than that for NG-P150, NG-P100 and G-P300. For example, the values of C_{sc} for NG-P100, NG-P150, NG-P300 and G-P300 are about 3.55, 1.45, 1.32 and 1.65 mFcm^{-2} at scan rate of 1.0 Vs^{-1} , and about 0.60, 0.64, 0.84 and 0.47 mFcm^{-2} at scan rate of 50 Vs^{-1} , respectively. The C_{sc} value can still retains 36.6% (0.47 mFcm^{-2}) for NG-P300, 21.2% (0.30 mFcm^{-2}) for NG-P150, 7.29% (0.26 mFcm^{-2}) for NG-P100 and 10.3% (0.17 mFcm^{-2}) at the scan rate of 800 Vs^{-1} . The higher C_{sc} value for NG-P300 at large scan rate also indicates that the it exhibits better potential for use in ultra-fast electrochemical capacitor than NG-P150 and NG-P100. The C_{sc} of the electrodes is usually depended on the specific surface area, functional groups and doping of the materials of electrodes. It is considered that the pyridinic type of N plays a important role for the improved capacitances for all electrolytes and the pyrrolic type of N can improve the capacitance further when negatively charged and that the presence of quaternary-type of N can improve the conductivity of graphene [37], which will causes NG-P's specific capacitance larger. The capacitors assembled by films of NG-P300 with different thicknesses have been also measured by electrochemical method. The results show that the capacitors possess almost the same specific capacitance at high scan rates (Fig. S9) although the films of NG-P300 have different thicknesses. This indicates that the formed films are compact and that the specific capacitance of the films mainly depends on the geometric surface area of the materials. The charging/discharging curves at large current density (Fig. S10) show the capacitor fabricated by NG-P300 with a thickness of 4 μm has a very small iR drop, and that the C_{sc} calculated on the basis of discharging curves slightly decrease and found to be about 613, 606, 601, 597 and 592 μFcm^{-2} at the current densities of 200, 500, 800, 1000 and 1500 μAcm^{-2} , respectively.

Fig. 11A shows the complex plot obtained at the frequency-range of 10^5 - 10^{-2} Hz (the inserted figure shows the high-frequency region). The nearly vertical slope of each plot indicates a good capacitor behavior of the cells. The negligible high-frequency resistor-capacitor loop indicates a good electrode contact and the non-microporous structure [34,38]. Furthermore, the capacitor assembled by NG-P300 shows the smallest equivalent series resistances. From the plots of the capacitance of the capacitors versus the frequency (Fig. 11B), it is easy to find that the capacitors assembled by NG-P300, NG-P150, NG-P100 and G-P300 have a capacitance of about 0.318, 0.224, 0.216 and 0.157 mFcm^{-2} at 120Hz, respectively. According to literature [35], the resistor-capacitor (RC) time

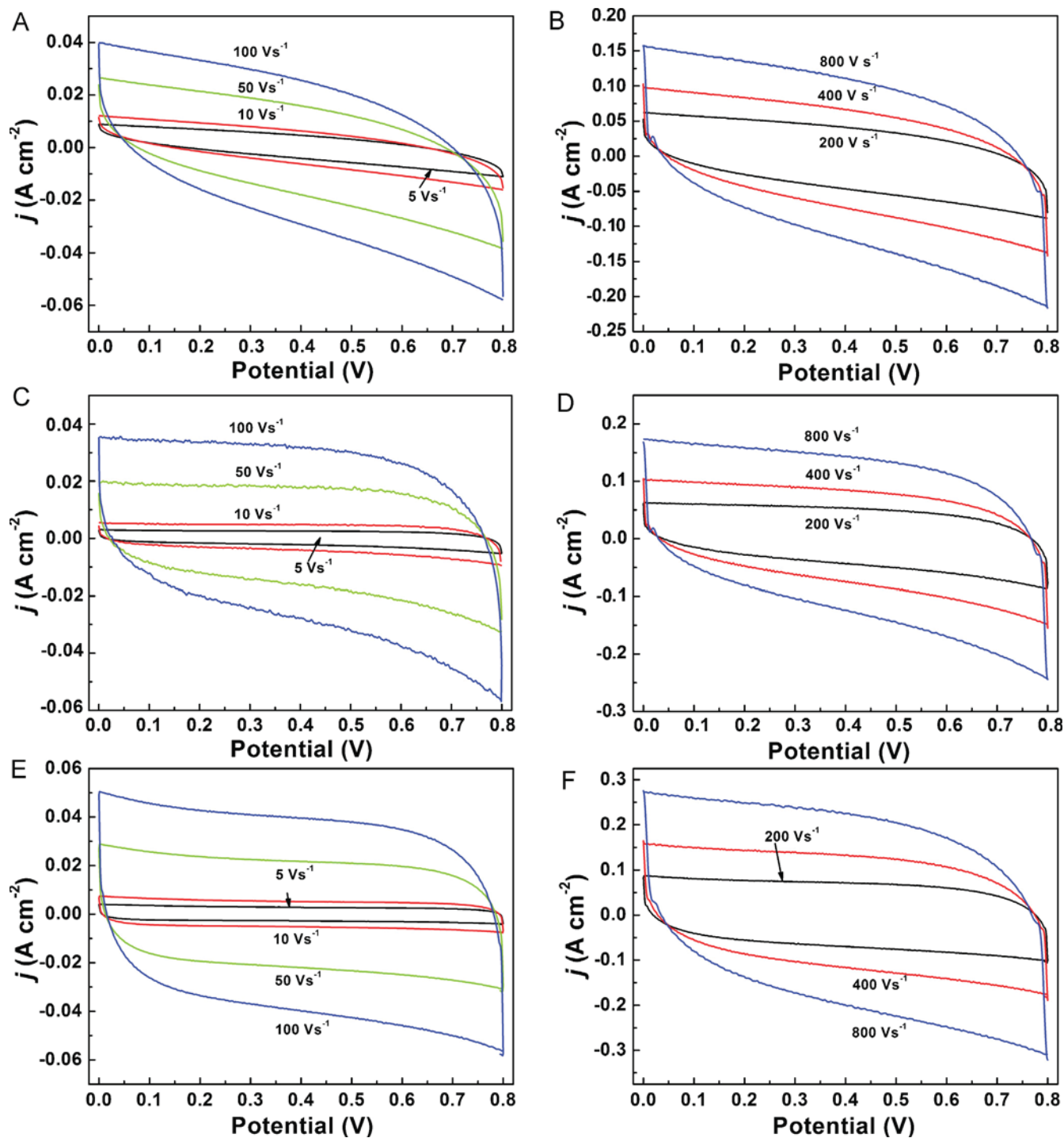


Figure 8. The CV curves of the capacitors assembled by NG-P at different scan rates, NG-P100 (A and B), NG-P150 (C and D) and NG-P300 (E and F).

constant of the capacitors fabricated by NG-P300 and NG-P150 are calculated to be about 1.40 and 1.43 ms according to the data at 120 Hz. As shown in Fig. 11 C, the prototype capacitors fabricated by NG-P300, NG-P150, NG-P100 and G-P300 have the impedance phase angle of -77.1° , -71.4° , -59° and 62.5° at 120 Hz respectively, which indicates that the capacitor fabricated by NG-P300 has better ultrahigh-rate capacitive properties used for ac line-filtering. The impedance phase angle of -77.1° for capacitor of NG-P300 is slightly smaller than that of vertical graphene nanosheet capacitor (-82°) and aluminum electrolytic capacitor (-83°) but much larger

than that of activated carbon capacitor [34]. The impedance phase angle of the capacitor assembled by NG-P300 reaches -45° at about 20000 Hz, which is larger than 15000 Hz for the capacitor of the vertical graphene sheets and 0.15 Hz for the activated carbon capacitor but lower than 30000 Hz for the aluminum electrolytic capacitor. According to the EIS measurements, it is considered that the capacitor fabricated by NG-P300 have the ultra-high capacitive properties [36]. Take into account that the thickness of NG-P300 is $4.0 \mu\text{m}$ and the thickness of active material in the capacitor is about $8.0 \mu\text{m}$, and that specific capacitance at 120 Hz for capacitor is about 0.318 mF

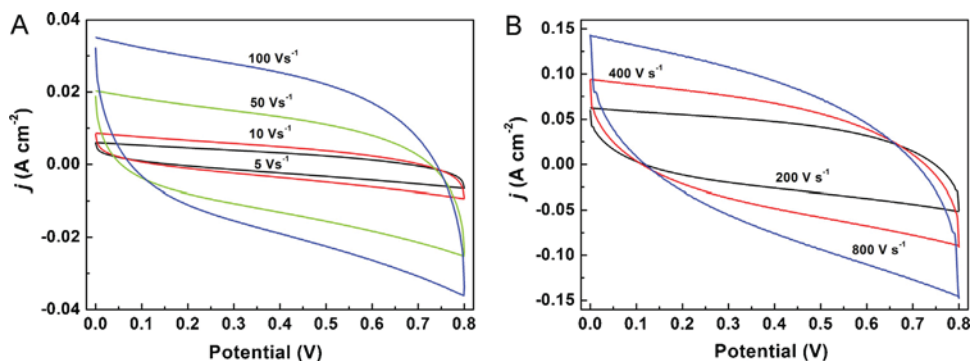


Figure 9. The CV curves of the capacitors assembled by G-P300 at different scan rates.

cm^{-2} , then the capacitance density can be calculated to be about 0.4 F cm^{-3} and the value of capacitance density \times voltage is about 0.32 FV cm^{-3} which is larger than that low-voltage aluminum anode foil (0.14 FV cm^{-3}).

The capacitive properties of NG-MWCNT-P have also been simply measured although the NG-MWCNT-P prepared here is mainly to verify the effectiveness of DIA for composite films. It is found that the CV curves of the cells can maintain the quasi-rectangular shape at scan rate of 1.0 V s^{-1} (Fig.S11) but the C_{CS} value of NG-MWCNT-P100 can only reach 90.0 F g^{-1} at scan rate of 5.0 mV s^{-1} , which may be attributed to the small C_{CS} of MWCNTs [39] and content of MWCNTs (CNTs: GO = 1: 4 in weight for preparation) is not the optimum. The C_{CS} values of NG-MWCNT-P100 decrease with the increment of scan rates (Fig. 12A), but the C_{CS} can retain 55.6% of its initial capacitance at scan rate of 1.0 V s^{-1} , which is much better than many previously reported carbon materials [40–43]. Fig. 12B presents the plots of the phase angle versus the frequency of the capacitors assembled by NG-MWCNT-P100. It is known that the characteristic frequency f_0 for phase angle of -45° marks the point at which the resistive and capacitive impedances are equal [44]. The f_0 can provide a time constant τ_0 ($1/f_0$) which tells how fast the device can be reversibly charged and discharged [45,46]. It is found that the τ_0 for capacitor of NG-MWCNT-P100 is about 0.14 s , which is much smaller than that of porous carbon nanofibers film electrodes prepared by electrospinning (0.47 s) [45] and the mesoporous carbon synthesized by silica-assisted strategy [40]. This indicates that

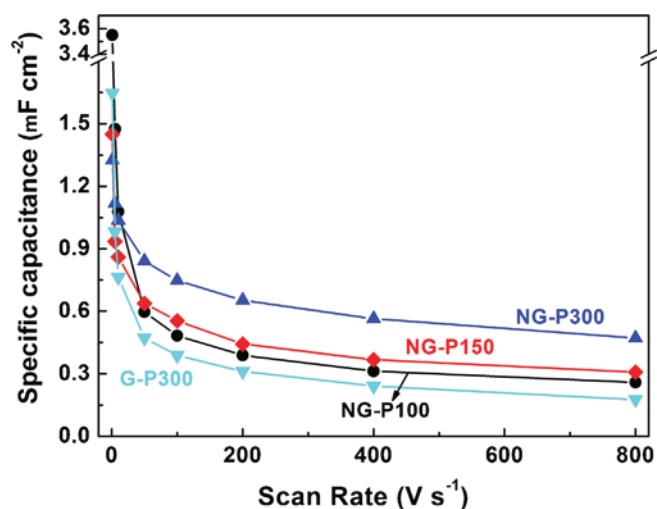


Figure 10. The plots of the specific capacitance for NG-P and G-P300 versus scan rates.

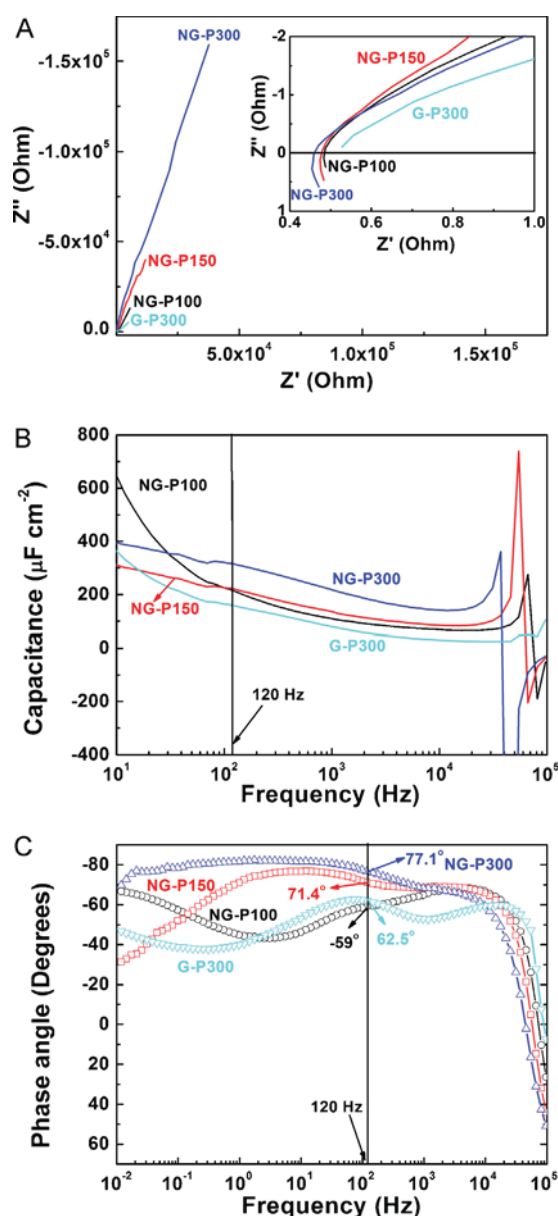


Figure 11. The complex plots of the EIS of the cell assembled by the NG-P and G-P300 (A, the insertion is the region of high-frequency part), the plots of the capacitance of the capacitors fabricated by NG-P and G-P300 versus the frequency (B) and the plots of the impedance phase angles versus the frequency (C).

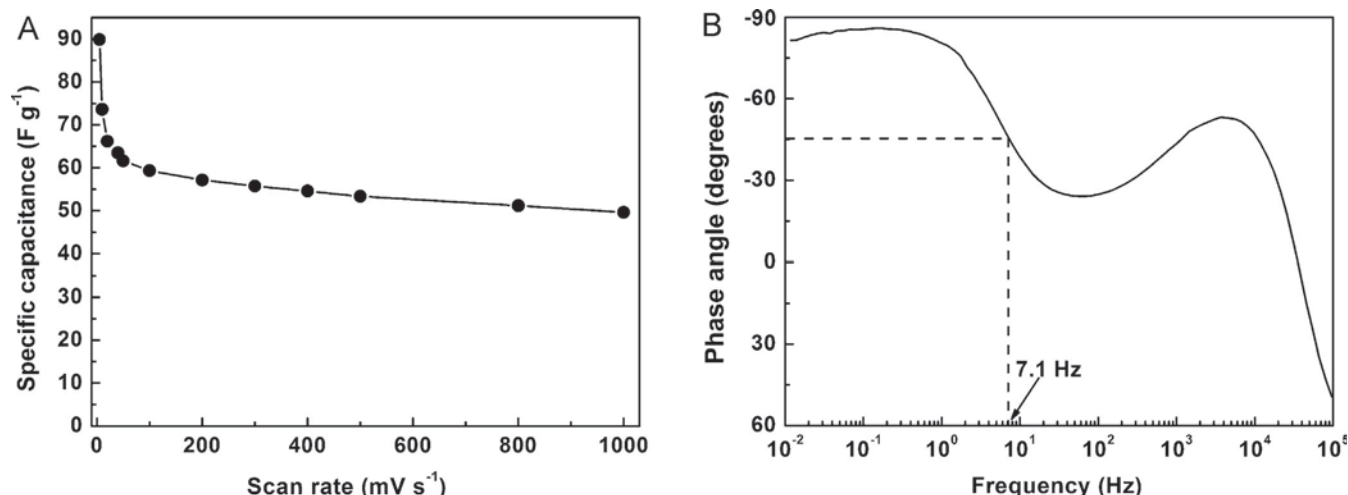


Figure 12. The plots of the specific capacitance of NG-MWCNT-P100 versus the scan rates (A) and the phase angle versus the frequency (B).

NG-MWCNT-P exhibits the high rate capability although the C_{cs} is not much large.

4. Conclusions

Different from the preparation of the graphene-based material such as filtration, spinning coat and hydrothermal method *etc.*, we have prepared the NG-P and NG-MWCNT-P in large-scale by using DIA process, during which the molding of GO is carried out at room temperature, the reduction of GO and the N-doping are achieved simultaneously under atmospheric pressure and at low temperature. The obtained NG-P exhibits good mechanical, electrical conductivity, thermal conductivity and ultra-high capacitive performance and may exhibit use in the field of ac line-filtering. The obtained composite of NG-MWCNT-P exhibit high rate capability although the C_{cs} is not large. This method provides a facile approach to prepare various N-doped graphene-based films in large-scale, and may be applied to other fields such as molecular or nano-materials assembly, composite materials *etc.*

Acknowledgements

We appreciate funding from National Natural Science Foundation of China (21274082 and 21073115) and Shanxi province (2012021021-3), and the Program for New Century Excellent Talents in University (NCET-10-0926).

Appendix A. Supplementary data

Supplementary data associated with this article can be found, in the online version, at <http://dx.doi.org/10.1016/j.electacta.2013.10.203>.

References

- [1] K.S. Novoselov, A.K. Geim, S.V. Morozov, D. Jiang, Y. Zhang, S.V. Dubonos, I.V. Grigorieva, A.A. Firsov, Electric field effect in atomically thin carbon films, *Science* 306 (2004) 666.
- [2] S. Stankovich, D.A. Dikin, G.H.B. Dommett, K.M. Kohlhaas, E.J. Zimney, E.A. Stach, R.D. Piner, S.T. Nguyen, R.S. Ruoff, Graphene-based composite materials, *Nature* 442 (2006) 282.
- [3] Y.Y. Liu, G.Y. Han, Y.L. Li, M. Jin, Flower-like zinc oxide deposited on the film of graphene oxide and its photoluminescence, *Mater. Lett.* 65 (2011) 1885.
- [4] D.Y. Fu, G.Y. Han, Y.Z. Chang, J.H. Dong, The synthesis and properties of ZnO-graphene nano hybrid for photodegradation of organic pollutant in water, *Mater. Chem. Phys.* 132 (2012) 673.
- [5] J.H. Fang, M. Li, Q.Q. Li, W.F. Zhang, Q.L. Shou, F. Liu, X.B. Zhang, J.P. Cheng, Microwave-assisted synthesis of CoAl-layered double hydroxide/graphene oxide composite and its application in supercapacitors, *Electrochim. Acta* 85 (2012) 248.
- [6] E. Yoo, T. Okata, T. Akita, M. Kohyama, J. Nakamura, I. Honma, Enhanced electro-catalytic activity of Pt subnanoclusters on graphene nanosheet surface, *Nano Lett.* 9 (2009) 2255.
- [7] Y.Z. Chang, G.Y. Han, M.Y. Li, F. Gao, Graphene-modified carbon fiber mats used to improve the activity and stability of Pt catalyst for methanol electrochemical oxidation, *Carbon* 49 (2011) 5158.
- [8] X. Wang, L.J. Zhi, K. Mullen, Transparent, Conductive graphene electrodes for dye-sensitized solar cells, *Nano Lett.* 8 (2008) 323.
- [9] W.J. Hong, Y.X. Xu, G.W. Lu, C. Li, G.Q. Shi, Transparent graphene/PEDOT-PSS composite films as counter electrodes of dye-sensitized solar cells, *Electrochim. Commun.* 10 (2008) 1555.
- [10] M.D. Stoller, S.J. Park, Y.W. Zhu, J.H. An, R.S. Ruoff, Graphene-based ultracapacitors, *Nano Lett.* 8 (2008) 3498.
- [11] X. Du, P. Guo, H.H. Song, X.H. Chen, Graphene nanosheets as electrode material for electric double-layer capacitors, *Electrochim. Acta* 55 (2010) 4812.
- [12] Q.L. Du, M.B. Zheng, L.F. Zhang, Y.W. Wang, J.H. Chen, L.P. Xue, W.J. Dai, G.B. Ji, J.M. Cao, Preparation of functionalized graphene sheets by a low-temperature thermal exfoliation approach and their electrochemical supercapacitive behaviors, *Electrochim. Acta* 55 (2010) 3897.
- [13] C. Lee, X.D. Wei, J.W. Kysar, J. Hone, Measurement of the elastic properties and intrinsic strength of monolayer graphene, *Science* 321 (2008) 385.
- [14] A.S. Mayorov, R.V. Gorbachev, S.V. Morozov, L. Britnell, R. Jalil, L.A. Ponomarenko, P. Blake, K.S. Novoselov, K. Watanabe, T. Taniguchi, A.K. Geim, Micrometer-scale ballistic transport in encapsulated graphene at room temperature, *Nano Lett.* 11 (2011) 2396.
- [15] A.A. Balandin, Thermal Properties of graphene and nanostructured carbon materials, *Nature Mater.* 10 (2011) 569.
- [16] H. Bai, G.Q. Shi, Functional composite materials based on chemically converted graphene, *Adv. Mater.* 23 (2011) 1089.
- [17] P.W. Sutter, J.I. Flege, E.A. Sutter, Epitaxial graphene on ruthenium, *Nature Mater.* 7 (2008) 406.
- [18] K.S. Kim, Y. Zhao, H. Jang, S.Y. Lee, J.M. Kim, K.S. Kim, J.H. Ahn, P. Kim, J.Y. Choi, B.H. Hong, Large-scale pattern growth of graphene films for stretchable transparent electrodes, *Nature* 457 (2009) 706.
- [19] Y.X. Xu, H. Bai, G.W. Lu, C. Li, G.Q. Shi, Flexible graphene films via the filtration of water-soluble covalent functionalized graphene sheets, *J. Am. Chem. Soc.* 130 (2008) 5856.
- [20] C. Chen, Q.H. Yang, Y. Yang, W. Lv, Y. Wen, P.X. Hou, M. Wang, H.M. Cheng, Self-assembled free-standing graphite oxide membrane, *Adv. Mater.* 21 (2009) 3007.
- [21] C. Valles, J.D. Nunez, A.M. Benito, W.K. Maser, Flexible conductive graphene paper obtained by direct and gentle annealing of graphene oxide paper, *Carbon* 50 (2012) 835.
- [22] H. Wang, T. Maiyalagan, X. Wang, Review on recent progress in nitrogen-doped graphene: synthesis, characterization, and its potential applications, *ACS Catal.* 2 (2012) 781.
- [23] D. Wei, Y. Liu, Y. Wang, H. Zhang, L. Huang, G. Yu, Synthesis of N-Doped graphene by chemical vapor deposition and its electrical properties, *Nano Lett.* 9 (2009) 1752.
- [24] C.H. Zhang, L. Fu, N. Liu, M.H. Liu, Y.Y. Wang, Z.F. Liu, Synthesis of nitrogen-doped graphene using embedded carbon and nitrogen sources, *Adv. Mater.* 23 (2011) 1020.
- [25] L.S. Panchakarla, K.S. Subrahmanyam, S.K. Saha, A. Govindaraj, H.R. Krishnamurthy, U.V. Waghmare, C.N.R. Rao, Synthesis, structure, and properties of boron- and nitrogen-doped graphene, *Adv. Mater.* 21 (2009) 4726.

- [26] D.S. Geng, Y. Chen, Y.G. Chen, Y.L. Li, R.Y. Li, X.L. Sun, S. Ye, S. Knights, High oxygen-reduction activity and durability of nitrogen-doped graphene, *Energy Environ. Sci.* 4 (2011) 760.
- [27] D.H. Long, W. Li, L.C. Ling, J. Miyawaki, I. Mochida, S.H. Yoon, Preparation of nitrogen-doped graphene sheets by a combined chemical and hydrothermal reduction of graphene oxide, *Langmuir* 26 (2010) 16096.
- [28] L.F. Lai, L.W. Chen, D. Zhan, L. Sun, J.P. Liu, S.H. Lim, C.K. Poh, Z. Shen, J. Lin, One-step synthesis of NH_2 -graphene from in situ graphene-oxide reduction and its improved electrochemical properties, *Carbon* 49 (2011) 3250.
- [29] L. Sun, L. Wang, C.G. Tian, T.X. Tan, Y. Xie, K.Y. Shi, M.T. Li, H.G. Fu, Nitrogen-doped graphene with high nitrogen level via a one-step hydrothermal reaction of graphene oxide with urea for superior capacitive energy storage, *RSC Adv.* 2 (2012) 4498.
- [30] D. Li, M.B. Muller, S. Gilje, R.B. Kaner, G.G. Wallace, Processable aqueous dispersions of graphene nanosheets, *Nature Nanotechnol.* 3 (2008) 101.
- [31] Y.Z. Chang, G.Y. Han, J.P. Yuan, D.Y. Fu, F.F. Liu, S.D. Li, Using hydroxylamine as a reducer to prepare N-doped graphene hydrogels used in high-performance energy storage, *J. Power Sources* 238 (2013) 492.
- [32] D.R. Dreyer, S.J. Park, C.W. Bielawski, R.S. Ruoff, The chemistry of graphene oxide, *Chem. Soc. Rev.* 39 (2010) 228.
- [33] Y. Wang, Y.Y. Shao, D.W. Matson, J.H. Li, Y.H. Lin, Nitrogen-doped graphene and its application in electrochemical biosensing, *ACS Nano* 4 (2010) 1790.
- [34] J.R. Miller, R.A. Outlaw, B.C. Holloway, Graphene double-layer capacitor with ac line-filtering performance, *Science* 329 (2010) 1637.
- [35] K.X. Sheng, Y.Q. Sun, C. Li, W.J. Yuan, G.Q. Shi, Ultrahigh-rate supercapacitors based on electrochemically reduced graphene oxide for ac line-filtering, *Sci Rep.* 2 (2012) 247.
- [36] J.R. Miller, R.A. Outlaw, B.C. Holloway, Graphene electric double layer capacitor with ultra-high-power performance, *Electrochim. Acta* 56 (2011) 10443.
- [37] H.M. Jeong, J.W. Lee, W.H. Shin, Y.J. Choi, H.J. Shin, J.K. Kang, J.W. Choi, Nitrogen-doped graphene for high-performance ultracapacitors and the importance of nitrogen doped sites at basal planes, *Nano Lett.* 11 (2011) 2472.
- [38] L.L. Zhang, X. Zhao, M.D. Stoller, Y.W. Zhu, H.X. Ji, S. Murali, Y. Wu, S. Peralas, B. Clevenger, R.S. Ruoff, Highly conductive and porous activated reduced graphene oxide films for high-power supercapacitors, *Nano Lett.* 12 (2012) 1806.
- [39] M.H. Ervin, B.S. Miller, B. Hanrahan, B. Mailly, T. Palacios, A comparison of single-wall carbon nanotube electrochemical capacitor electrode fabrication methods, *Electrochim. Acta* 55 (2012) 37.
- [40] Z.A. Qiao, B.K. Guo, A.J. Binder, J.H. Chen, G.M. Veith, S. Dai, Controlled synthesis of mesoporous carbon nanostructures via a silica-assisted strategy, *Nano Lett.* 13 (2013) 207.
- [41] M.J. Zhong, E.K. Kim, J.P. McGann, S.E. Chun, J.F. Whitacre, M. Jaroniec, K. Matyjaszewski, T. Kowalewski, Electrochemically active nitrogen-enriched nanocarbons with well-defined morphology synthesized by pyrolysis of self-assembled block copolymer, *J. Am. Chem. Soc.* 134 (2012) 14846.
- [42] P.Q. Wang, D. Zhang, F.Y. Ma, Y. Ou, Q.N. Chen, S.H. Xie, J.Y. Li, Mesoporous carbon nanofibers with a high surface area electrospun from thermoplastic polyvinylpyrrolidone, *Nanoscale* 4 (2012) 7199.
- [43] B.H. Kim, K.S. Yang, J.P. Ferraris, Highly conductive, mesoporous carbon nanofiber web as electrode material for high-performance supercapacitors, *Electrochim. Acta* 75 (2012) 325.
- [44] P.L. Taberna, P. Simon, J.F. Fauvarque, Electrochemical characteristics and impedance spectroscopy studies of carbon-carbon supercapacitors, *J. Electrochem. Soc.* 150 (2003) 292.
- [45] C. Ma, Y. Song, J.L. Shi, D.Q. Zhang, X.L. Zhai, M. Zhong, Q.G. Guo, L. Liu, Preparation, one-step activation of microporous carbon nanofibers for use as supercapacitor electrodes, *Carbon* 51 (2013) 290.
- [46] L. Zhang, G.Q. Shi, Preparation of highly conductive graphene hydrogels for fabricating supercapacitors with high rate capability, *J. Phys. Chem. C* 115 (2011) 17206.